SPICAM and SPICAV data level 1A IR
Process description

Version	Date	Comments
1	19/12/2014	First release
2	21/07/2015	Updated parts 4.1 and 4.4

Prepared by:	Approved by:
NICOLAS CHAPRON **SVETLANA GUSLYAKOVA**	**ANNA FEDOROVA**

1 Introduction

1.1 Purpose

This document provides a description for the different process applied on the raw SPICAM and SPICAV IR data to obtain the level 1A. Concatenated with the geometry, the data in the level 1A is corrected from the missing packets, the dark current and the RF-wavelength calibration is applied. The algorithm of wavelength-geometry correlation is also presented.

1.2 Reference documents

Ref N°	Title	Author	Date
1	otchet_express_vex_mars2013_v8.doc	Anna Fedorova	19/12/2011
2	SPICAM IR acousto-optic spectrometer experiment on Mars Express	Korablev et al.	J. Geophys. Res. 111 (E9), 2006
3	Exploration of Mars in SPICAM-IR experiment onboard the Mars-Express spacecraft: 1. Acousto-optic spectrometer SPICAM-IR	Korablev et al.	Cos. Res. 44 (4), 278-293 2006
4	SPICAV IR acousto-optic spectrometer experiment on Venus Express	Korablev et al.	Planet. Space Sci. 65 (1), 38-57

1.3 Abbreviations

ADC	Analog-to-digital converter
ADU	Analog to Digital Unit
AOTF	Acousto-optical tunable filter
DC	Dark Current
DDS	Data Distribution System
FITS	Flexible Image Transport System
FWHM	Full Width at Half Maximum
IR	Infrared
LW	Long Wavelength Channel
MEx	Mars-Express
NaN	Not a Number
RF	Radio frequency
SPICAM	Spectroscopy for Investigation of Characteristics of the Atmosphere of Mars
SPICAV	Spectroscopy for Investigation of Characteristics of the Atmosphere of Venus
SW	Short Wavelength Channel
VEx	Venus-Express

2 Overall overview of the process

The following diagram represents an overall overview of the correction process:

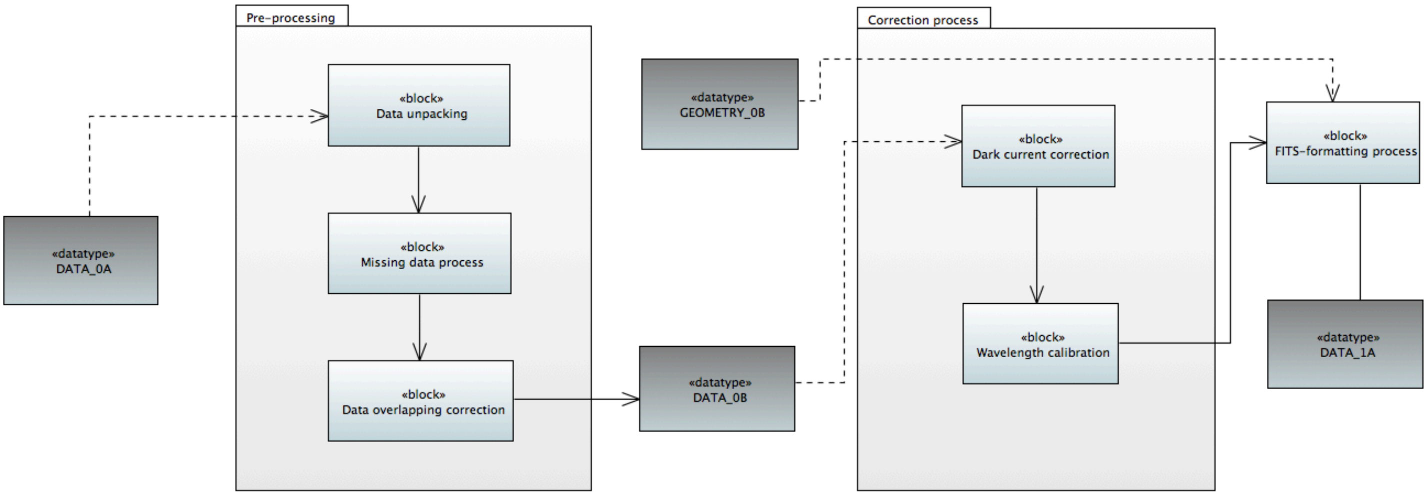

3 Pre-processing

3.1 FITS formatting

In the level 0B (raw), the data and geometry are available in two different files. For convenient use, both data and geometry are concatenated in one file under the FITS[1] format. The benefit of this format is the flexibility to add several image extensions.

3.2 Missing data processing

SPICAM and SPICAV observations can have missing packets due to the communication troubles between the satellite and the earth ground segment. The presence of missing packets in an observation causes a wrong total number of records (or spectra). Two spectra can be consecutive but are in fact separated by a certain gap time corresponding to missing data. This process purpose is to inject empty values to retrieve the correct number of records.

The criterion to look for gaps is the record time. New lines, corresponding to the detected missing records, are injected with NaN[2] values in the data array, for all the spectral points in the missing packet.

[1] *FITS: Flexible Image Transport System*
[2] *NaN: Not a Number, data type representing an undefined value, IEEE 754 standard*

4 Correction process description

4.1 Data overlapping correction

4.1.1 *Correction for SPICAM IR:*

All measurement data (Data and System monitor fields) originate from the output of controller 12 bit ADC (Analog-to-digital converter). The ADC operates in +/- 5V full-scale bipolar mode and its output is twos-complement binary code:

Value	Binary code
+2047	0111 11111111b
…	
+1	0000 00000001b
0	0000 00000000b
-1	1111 11111111b
…	
-2048	1000 00000000b

Table 4-1 : Correspondance between ADU and Binary code

The ADC data obtained in channels of photodetectors are processed afterwards. The following integer operations are performed:
- A sum of N ADC measurements of the signal with AOTF on is accumulated,
- Another sum of N ADC measurements of the signal with AOTF off is accumulated,
- Difference between these two sums is calculated,
- The difference is normalized (divided by N),
- 12 LSBs of the result is the data point.

Addition and division operations compensate each other in the sense that they do not change output numbers range compared to the input 12bits range. But subtraction is not compensated and doubles the output range – in fact data points are 13bit signed integer values. Since only 12LSbits are transmitted the sign bit of data points is truncated.
In result when the signal begins to grow and reaches 2048, it falls to -2048 and continues to grow again in negative units. This must be taken into account when treating the device data.

The first correction of the data overlapping is computed with the following formula:

$$S_i(f) = 4096 + S_i(f) \quad if\ S_i(f) < -1000$$

Where $S_i(f)$ is a signal of ***i*** channel at frequency *f* in ADU.

4.1.2 *Correction for SPICAV IR:*

The same problem exists for the SPICAV IR channel. During observations of solar occultation and nadir observations with small SZA (<40) the signal in ADU of SW channel can exceed values of 5000 and even 7000. The data is cut off to 12 bit digital signed word. So if the value is:

- $A=5000$, it will be $A_{sp}=904$,
- $B=3500$, it will be $B_{sp}=-596$.

The conversion of data to real digital value has to be done before the calibration of IR channel. If a full spectrum was recorded the correction is computed with following formula:

$$S_i(f) = 4096 + S_i(f) \quad if\ S_i(f) < -100 \text{ and TIME<3ms and } f\text{>140 MHz (SW channel)}$$

$$S_i(f_{i+1}) = 4096 + S_i(f_{i+1}) \quad if\ (S_i(f_i) - (S_i(f_{i+1})) > 3500$$

Where

- $S_i(f)$ is a signal of ***i*** channel at frequency *f* in ADU
- TIME is the AOTF integration period
- *f* is the radio frequency in MHz.

The algorithm is more difficult for the DOTS set. The set of DOTS can be found in the *commands-configs-FM2b_XXXX_xxx.xls* file. The sets have been fixed before the flights and can't be changed. 4 spectral points of the SW channel are used in the DOTS set. Flight configurations 4 and 7 are used all the time with these 4 points. The new special algorithm for these DOTS has been developed and implemented for TIME<3 msec. The algorithm takes into account relative variations of solar intensity and detector's sensitivity between SW points separates up to 100 nm. It is not worked for any other sets of SW DOTS, but due to only this set was regularly used we have not pay attention to the more common algorithm.

4.2 Dark Current correction

4.2.1 Correction for SPICAM IR

The measurements of the AOTF spectrometer are based on digital synchronous detection, and for each measurement the dark signal is subtracted from the useful signal. Still, some background signal may propagate owing to synchronized optical or electrical interference. The synchronized RF interference from the AOTF driver was significant for the Mars version of the instrument, forming a characteristic pattern in function of wavelength [3, 4].

This kind of interference depends on radio frequency (RF) and power, and forms a characteristic pattern as a function of wavelength. This pattern, well characterized on the ground, has changed after the launch with a minimum, which appeared around 1.35 µm. Also, we have noticed slight modifications of the background as a function of the observation mode (Nadir, Limb, etc.), due, most likely to the modification of the thermal regime. A special effort has been dedicated to characterize the background behavior in flight, as a function of particular observation modes, and including the dependence on temperature and other parameters. To support this study, the IR spectrometer is maintained on during most of operations when no significant signal in the IR is expected.

As soon as the background signal is determined, the correction procedure is trivial and consists of subtraction of the averaged smoothened background signal ("Dark Current" (DC)) from each measured spectrum. The radiation coming from the planet can be presented as:

$$S = M - D$$

Where

- M is a measured signal
- S is a source signal
- D is a dark current

The DC has a temperature and RF dependence. Depending on the command set, there are several formulations to estimate the dark current: constant, linear and quadratic polynomial approximation, as shown in the following table:

Case	DAC	GAIN	TIME [ms]	Dark Current
1	1744	8.25	5.6	$D_g(f)=a_d(f)\times T^2+b_d(f)\times T+c(f)$
2	1504	3.0	5.6	$D_g(f)=a_d(f)\times T+b_d(f)$
3	1744	3.0	2.8	$D_g(f)=a_d(f)$

Table 4-2 : Formulations of the Dark Current estimation

Where

- TIME is the AOTF integration period.
- GAIN is the amplifiers gain factor.
- DAC is the AOTF RF power control
- D_g is the dark signal in ADU/gain factor
- T is the temperature of detectors in Volts
- f is the radio frequency in MHz.

The coefficients a, b and c are given for sequence of frequencies~~y~~ from 84 to 147 MHz with step 0.5 MHz for cases 1 and 2 and step 0.192 MHz for case 3. The coefficients are different for detectors 0 and 1.

The first case (DAC=1744, GAIN = 8.25, TIME = 5.6 ms) is a main mode of nadir observation. Finally, the DC for each frequency could be obtained as

$$S(f) = M(f) - D_g(f) \times GAIN$$

4.2.2 Correction for SPICAV IR:

For SPICAV the DC is much weaker compared to SPICAM but still it has to be taken into account during the data treatment especially for low signal. The cooling of the detectors substantially decreases the DC and noise and it is preferentially used in flight [5].

A special effort has been dedicated to characterize the background behaviour in flight, as a function of particular observation modes, detector's temperature, integration time and gain. To support this study, the IR spectrometer was powered in the most practical observation regimes during several orbits when no significant signal in the IR was expected (e.g., while SPICAV UV observes in stellar occultation mode~~s~~, away from the planet's disk).

1) The DC was measured for 3 main commands and Peltier on and off:
   - TIME=2.8 ms, GAIN=8
   - TIME=89.6 ms, GAIN=8
   - TIME=89.6 ms, GAIN=16.
2) DC is significantly different for the two polarizations (Channels 0 and 1) owing to different electrical interference.
3) the DC is lower in the SW channel, while in the LW channel it is more variable.
4) The DC and its variations are especially important for the observations of weak signals on the nightside.
5) For the dayside observations the DC can be considered insignificant both for LW and SW channels. On the other hand, a good knowledge of the background for both detectors is a must for polarization studies on the dayside, when the difference of two polarizations can be less than 1%.

As soon as the background signal is determined for each TIME and GAIN, the correction procedure is trivial and consists of subtraction of the averaged smoothened background signal from each measured spectrum:

$$S = M - D$$

4.3 Wavelength calibration

The tuning curve of an AOTF can be described as $\lambda \sim \frac{a}{f}$. The dispersion of the AOTF crystal changes with temperature, and the wavelength assignment of the AOTF spectrometer is expected to change with the drift of the crystal temperature owing to internal heat dissipation or environmental conditions (relative wavelength shift is ~$1.6 \cdot 10^{-2}$ nm K^{-1}). The AOTF unit is equipped with a sensitive temperature sensor in the proximity of the crystal.

4.3.1 Calibration for SPICAM IR:

We treat temperature as a quadratic perturbation to both coefficients *a* and *b*:

$$a, b = x + yt + z\,t^2$$

Where coefficients *x, y*, z are listed in the **Erreur ! Source du renvoi introuvable.**. The dispersion curve parameterized as:

$$\lambda = a/f + qf^2 + b \qquad \textit{for channel 0}$$

$$\lambda = a/f + b, \qquad \textit{for channel 1}$$

Where

- $q = -6.53\ 10^{-11}$
- λ is the wavelength expressed in nanometers
- *f* is the frequency in kHz
- *t* is the temperature measured by the sensor in degrees Celsius.

The accuracy of this calibration is better than ±0.2-0.3 nm within the range of 1100-1600 nm.

	X	*y*	*z*
Channel 0			
a	$1.367\ 10^{8}$	0	0
b	74.43	0.0285	10^{-4}
Channel 1			
a	$1.3690971\ 10^{8}$	2464.6217	–3.6228649
b	71.220396	$4.4824233\ 10^{-3}$	$-5.4920304\ 10^{-6}$

Table 4-3 : Fit coefficients for the wavelengths calibration curve.

And in the units of wavenumber it can be approximated as:

$$\nu = af^2 + bf + c, \qquad (1)$$

Where:

- ν is the wavenumber expressed in cm^{-1}
- *f* is the frequency in kHz.

4.3.2 Calibration for SPICAV IR:

The typical temperature of SPICAV in-flight is around –10°C varying from –21° to –4°C. The calibration with solar lines for AOTF temperature of –10°C was accepted as a reference. The coefficients *a, b*, c of the equation for the in-flight calibration are listed in the Table 4.3.2 for both channels and detectors. The dispersion is slightly different for two output polarizations of the AOTF (channels 0 and 1). The accuracy of this calibration is better than ±0.3 nm and ±0.5 nm within the LW and SW ranges respectively, including the uncertainty due to the temperature shift.

	a	*b*	*c*
Short wavelength channel (SW)			
Channel 0	-4.9405101e-008	7.6969006e-002	-2.9822051e+002
Channel 1	-5.0454785e-008	7.7358519e-002	-3.3244465e+002
Long wavelength channel (LW)			
Channel 0	-3.3865473e-008	7.2595705e-002	-2.0449838e+000
Channel 1	-3.5371703e-008	7.2919764e-002	-1.9140569e+001

Table 4-4 : Polynomial coefficients for the wavelengths calibration curve (Eq. 1)

4.4 Correlation of geometry and data points

4.4.1 Correlation for SPICAM IR:

SPICAM IR operates as point spectrometer and measures intensity at each wavelength sequentially. The sequence of AOTF frequencies (further converted into wavelengths) contains several blocks (usually 2 or 3) with 664 spectral points (332 pts for each detector) in each block. The time of the beginning of spectrum record (T_{sp}) is presented before each spectrum.

In course of measurement cycle the buffer is getting filled until one of the following conditions is met:

1. accumulated data fit the capacity of data blocks (in this case measurement is paused until data transfer),
2. measurement cycle is over,
3. command is received.

The geometry data also relates to defined time. So the correspondence between data and geometry is defined through the time of measurements. In geo data the first time corresponds to the beginning of first spectrum and time step corresponds to time of one block record:

TIME (ms)	Block size (sec)
2.8	1
5.6	2
11.2	4

The corresponding geometry can be found for each spectral point as

- N_{bl}=fix(n/332) (round to zero) – to find which block corresponds to this spectral point
- $T_{obs}=T_{sp}+N_{bl}*T_{bl}+(n-N_{bl}*332)*TIME*10^{-3}$; - to find exact time of the point

Where:

- T_{obs} is the time corresponding of the spectral point
- n is a number of spectral point
- TIME(ms) is the AOTF integration period

- N_{bl} – number of block in the spectrum (from 0)
- T_{bl} is the time of block record and transfer (2 sec for TIME=5.6 ms)

Example:
Typical solar occultation spectrum consists of 664 spectral points: 2 blocks and 4 sec totally. One spectral point takes 5.6 ms. T_{bl}=2 sec. The 1.43 μm H_2O band is located between 300 and 600 spectral points. Assume T_{sp}=0 sec
$T_{obs}(300)=0+0*2$ sec$+(300-0*332)*5.6\ 10^{-3}=1.68$ sec
$T_{obs}(600)=0+1*2$ sec$+(600-1*332)*5.6\ 10^{-3}=3.5$ sec

When the geometry for these times can be calculated from the interpolation with times in geo data and the geometry for the H_2O band should be averaged between these times.

The exact time of spectral point is especially important for limb measurements and solar occultations when the altitude of target point in the atmosphere changes with time. Users should take it into account when trying to find out the height corresponding to each spectral region.

4.4.2 Correlation for SPICAV IR:

The same reasoning should be taking into account for SPICAV IR except the geometry data are presented with step corresponding of the beginning of each spectrum and:

TIME (ms)	Block size (sec)
2.8	1
5.6	2
11.2	4
22.4	8
44.8	15
89.2	30